

Electrochemical and Quantum Chemical Study of Vanillin as a Green Corrosion Inhibitor for AA6061 in NaCl Solution

M. Shahidi^{1,*}, R. Mansouri², M.J. Bahrami² and S.M.A. Hosseini²

¹ Department of Chemistry, Kerman Branch, Islamic Azad University, Kerman, Iran

² Department of Chemistry, Shahid Bahonar University of Kerman, P.O. Box 76175-133, Iran

Received November 2014; Accepted December 2014

ABSTRACT

The effect of vanillin on the corrosion behavior of AA6061 Al alloy in 3.5% NaCl solution was investigated using potentiodynamic polarization and electrochemical noise (EN) techniques. Vanillin offers interesting possibilities for corrosion inhibition due to its nontoxicity and high solubility in aqueous media. The best inhibition effect at 200 ppm vanillin was a marked characteristic of the inhibitor. Potentiodynamic polarization measurements indicated that the inhibitor is of mixed type. According to calculated amount of noise charges by using the standard deviation of partial signal (SDPS) at the particular interval of frequency it is possible to obtain the inhibition efficiency of an inhibitor. The inhibition efficiency values obtained from EN method show a reasonable agreement with those obtained from potentiodynamic polarization measurements. According to the quantum chemical calculations it can be deduced that the number of intermolecular hydrogen bonds is increased by increase in concentration of vanillin. This verifies the decrease in the inhibition efficiency of vanillin at high concentrations.

Keywords: Vanillin; Electrochemical Noise; Wavelet Analysis; Natural Bond Orbital (NBO); Fukui Function

INTRODUCTION

Aluminum and its alloy represent an important category of materials due to their high technological value and wide range of industrial applications, especially in aerospace, household industries, automotive, transportation and marine technology. This is mainly because of their good specific strength, excellent formability and corrosion resistance. The corrosion resistance of aluminum arises from its ability to form a natural oxide film

on its surface in a wide variety of media, but the oxide film is readily susceptible to corrosion in chloride environments [1-4].

The use of inhibitors is one of methods for protection of materials against corrosion. Most well known inhibitors are organic compounds containing nitrogen, sulfur, and oxygen atoms. It is generally accepted that organic molecules inhibit corrosion by adsorption on metal surface. Though many organic compounds show

*Corresponding author: meshahidizandi@gmail.com

good anticorrosive activity, most of them are highly toxic. The investigation of new non-toxic or low-toxic and green corrosion inhibitors is essential to overcome this problem [5, 6].

Vanillin (4-hydroxy-3-methoxybenzaldehyde) is one of the most widely used and important flavoring materials worldwide. As shown in Fig. 1, aromatic ring of vanillin has three electron-withdrawing substituent groups then it can be adsorbed horizontally on the metal surface as a tripod inhibitor. It has many advantages such as low cost, non-toxicity and easy production [7]. In order to extend vanillin as corrosion inhibitor, this paper focus on the corrosion inhibition by vanillin for AA6061 aluminum alloy in 3.5% NaCl solution.

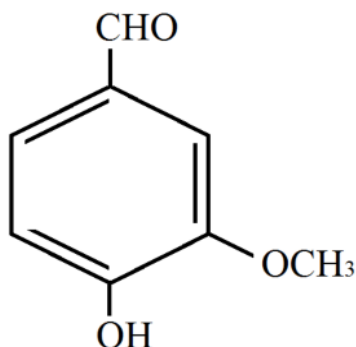


Fig. 1. The molecular structure of vanillin.

Potentiodynamic polarization curves and electrochemical noise (EN) methods were employed to evaluate corrosion of aluminum alloy and inhibition efficiency of the vanillin. Electrochemical noise is one of the most promising methods for monitoring and studying of corrosion processes [8]. Unlike the traditional electrochemical techniques (various types of potentiodynamic polarization tests,

impedance spectroscopy, etc.) EN measurements can be performed in freely corroding systems without the external application of electrical signals, so that the natural evolution of corrosion processes is assured. Furthermore, the traditional techniques can only be used to determine the general characteristics of corrosion systems, whereas the EN technique makes it possible to monitor corrosion evolution over time. EN is defined as the fluctuations of potential or current originating from the localized events in a corrosion process.

Wavelet transform is a mathematical tool to EN analysis [9]. Wavelet transform is regarded as a variant of Fourier transform that continuous waves used in the Fourier transform are replaced by transient waves with a finite duration. Wavelet transform produces $d1, d2, \dots, dJ$ (detail coefficients) and sJ (smooth coefficients) vectors termed crystals that include wavelet coefficients. Crystals describe the original signal on a different scale and the wavelet coefficients determine the similarity between the wavelet function and different segments of the signal.

The frequency range of each crystal is represented by the following equation:

$$(f_1, f_2) = (2^{-j} f_s, 2^{1-j} f_s) \quad (1)$$

where f_s is sampling frequency, and j is the number of crystal. The scale range of each crystal is given by:

$$(I_1, I_2) = (2^j \Delta t, 2^{j-1} \Delta t) \quad (2)$$

where Δt is sampling interval ($\Delta t = 1/f$). The frequency and scale range for $f_s = 4$ Hz are shown in Table 1.

Table 1. Frequency and scale range for $J = 7$ and $f_s = 4\text{Hz}$

Crystal name	d1	d2	d3	d4	d5	d6	d7
Scale range/s	0.25-0.5	0.5-1	1-2	2-4	4-8	8-16	16-32

The original signal can be reconstructed by adding the contributing wavelets weighted by their corresponding coefficients that known as inverse wavelet transform. Partial signal (PS) is a signal that resembles the fluctuations of the original signal at a particular interval of frequency [10]. For example PSD3 represents all fluctuations of the original signal between 1- 0.5 Hz, if the sampling frequency is 4 Hz. The standard deviation of partial signal (SDPS) is another method to present wavelet transform results that can indicate the variations in the intensity of the PS about its mean value which could be an indication of the intensity of electrochemical activity on the surface of the electrodes within a particular interval of frequency [11]. The plot of the SDPS versus their corresponding crystal name is called SDPS plot.

The present paper describes the study of the inhibition action of vanillin on corrosion of AA6061 Al alloy in 3.5% NaCl solution using potentiodynamic polarization and electrochemical noise techniques. In addition, quantum chemical computational such as natural bond orbital (NBO) and Fukui function were used to study the interaction between vanillin and the alloy surface. Quantum theory of atoms in molecules (QTAIM) analyze was also performed to investigate intermolecular hydrogen bonding in vanillin systems.

EXPERIMENTAL

Materials

Samples of type AA6061 aluminum alloy were coated in epoxy resin so that one flat face with an area of 1 mm² and 100 mm² were exposed to the solution. The specimens were connected to a copper wire at one end, and then sealed using epoxy resin with the other end exposed as the WE surface. Before performing experiments,

the WE surface was abraded by wet abrasive papers through 600–2500-grade, washed with distilled water, degreased with ethanol and finally dried in air. The electrodes were facing each other vertically at a distance of about 2 cm. A saturated (KCl) Ag/AgCl electrode was used as reference electrode. The counter electrode was a platinum wire.

Methods

Electrochemical noise experiments were conducted using Autolab 302N potentiostat with Nova 1.6 software. This equipment allows resolutions of 0.76 V for voltage signals and 10 nA for current signals. All the experiments were carried out in 3.5% NaCl solution without and with doping by different concentration of vanillin at 25 °C without passing any gas. Although EN studies tend to include both current and potential signals, this study concentrated on current signals only. The sampling frequency for the electrochemical noise data was 4 Hz. Noise data were analyzed with wavelet technique using the orthogonal Daubechies wavelets of the fourth order (db4). The necessary calculations for construction of the SDPS plots as well as the calculated signals were performed using Matlab software.

Potentiodynamic polarization curves were obtained by varying the applied potential from –250 up to +250 mV with respect to the open circuit potential (OCP) at a rate of 1 mV.s⁻¹. To obtain the stabilized OCP, the samples were immersed 30 min in the solution before measurements.

Computational details

To investigate the inhibition effect of vanillin on aluminum, the system of vanillin-Al was optimized within the Gaussian 03 package [12]. All calculations were carried out at the B3LYP/LanL2DZ

level and quantum theory of atoms in molecules (QTAIM) analysis was performed within AIM2000.

Molecular descriptors such as molecular orbital energy gap (Highest Occupied Molecular Orbital-Lowest Unoccupied Molecular Orbital: HOMO-LUMO), global hardness (η), global softness (S), electronegativity (χ), chemical potential (μ) and electrophilicity index (ω) were calculated for the optimized geometries [13].

The Fukui function defines the changes in electron number in chemical reactions and it has been used to predict the reactivity of sites in a molecule.

The f^+ and f^- (refer to an electrophile and a nucleophile, respectively) functions were used in this method that defined as:

$$f_k^+ = q_k^{(N+1)} - q_k^{(N)} \quad \text{For atom } k \text{ as an electrophile} \quad (3)$$

$$f_k^- = q_k^{(N)} - q_k^{(N-1)} \quad \text{For atom } k \text{ as a nucleophile} \quad (4)$$

The q_k is the electron population on atom k calculated in the systems with N , $N - 1$ and $N + 1$ electrons at the structure of the molecule with N electron [13, 14].

The theory of atoms in molecules (AIM) is based on a topological analysis of the electron density. The existence of a chemical bonding is characterized by a bond critical point (BCP) where properties of this point can show the nature of interaction. Value of electron density $\rho(r)$, Laplacian of electron density $\nabla^2\rho(r)$, kinetic energy density $G(r)$ and total energy density $H(r)$ are some properties of BCP which were utilized to consider the nature of interaction [15].

RESULTS AND DISCUSSION

Potentiodynamic polarization

Fig. 2 shows potentiodynamic polarization curves for AA6061 in 3.5% NaCl solution

containing various concentrations of vanillin. The corrosion parameters including corrosion current densities (i_{corr}), corrosion potential (E_{corr}), cathodic Tafel slope (b_c), anodic Tafel slope (b_a), and inhibition efficiency (IE%) are listed in Table 2.

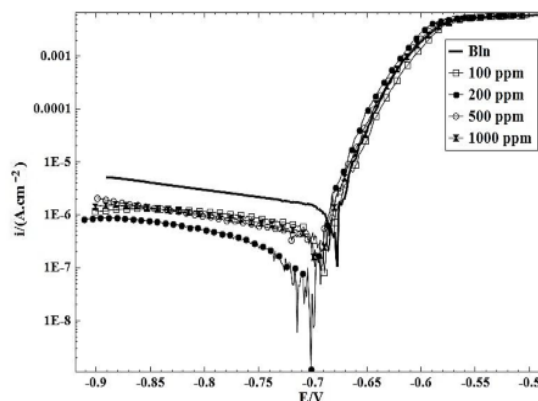


Fig. 2. Polarization curves of AA6061 in 3.5% NaCl solution in the absence and presence of different concentrations of vanillin at 25°C.

Addition of vanillin to NaCl solution affected both cathodic and anodic branches of the potentiodynamic polarization curves. Therefore, vanillin behaved as a mixed inhibitor. The results revealed that i_{corr} values decreased with increase in the concentrations of vanillin and the least i_{corr} value was obtained at 200 ppm of the vanillin. The corrosion inhibition efficiency is defined as:

$$IE \% = \frac{i_{\text{corr}} - i'_{\text{corr}}}{i_{\text{corr}}} \times 100 \quad (5)$$

where i_{corr} and i'_{corr} are corrosion current densities in the uninhibited and inhibited cases, respectively. It was observed that the inhibition efficiency increases with increasing concentration of the inhibitors up to 200 ppm. The highest inhibition efficiency reaches a maximum value of 88% at optimum concentration (200 ppm) of vanillin.

Electrochemical noise

Effect of inhibitor concentration

The EN measurements were used to

investigate the effect of vanillin as inhibitor on pitting corrosion of AA6061 in 3.5% NaCl. The EN current signals corresponding to two WEs with 1mm² and 100 mm² surface area in the absence and presence of different concentrations of vanillin are shown in Fig. 3. These signals were recorded after 25 minutes from the immersion time and during 300 s. Then the wavelet transform were used to analyze these signals and resulted SDPS plots are given in Fig. 4.

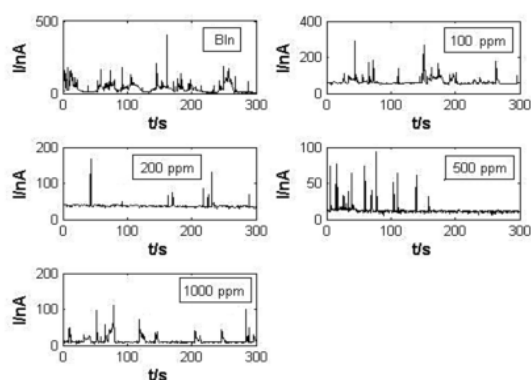


Fig. 3. EN current records of AA6061 in 3.5% NaCl solution in the absence and presence of different concentrations of vanillin during 300 s starting at 25 min after immersion time.

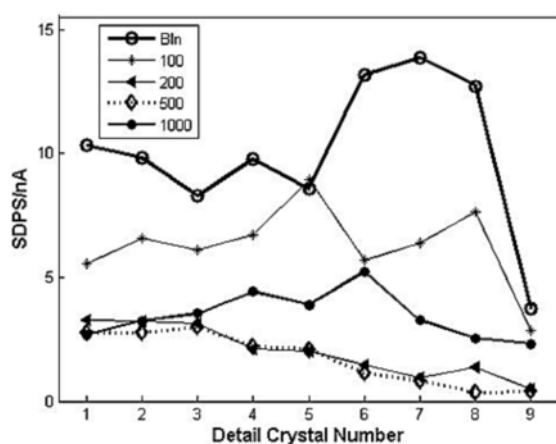


Fig. 4. SDPS plots of signals in Fig. 3.

The predominant transients can be attributed to metastable pits. The

development of a pit causes a quantity of electric charge to flow in the circuit which can be estimated by the following equation [16]:

$$Q = i_{\max} \cdot \tau_{\max} \quad (6)$$

where i_{\max} is the SDPS value at the maximum peak crystal (d_{\max}) and τ_{\max} is the average time width of d_{\max} crystal. Then it seems suitable to define the corrosion inhibition efficiency as follows:

$$IE_{EN} (\%) = \frac{Q - Q'}{Q} \times 100 \quad (7)$$

where Q and Q' are the noise charges in the uninhibited and inhibited cases, respectively.

It is evident from the SDPS plot of Signal Blank (Fig. 4) that the maximum is located at d4 crystal with the SDPS value of 9.7 nA (i_{\max}). According to Table 1, the average time width of crystal d4 is equal to 3 s. The values of the parameters derived from all the SDPS plots in Fig. 4 have been summarized in Table 3 (d_{\max} , τ_{\max} and i_{\max}). Table 3 also presents Q and IE values. These IE values are consistent with those obtained from potentiodynamic polarization (Table 2). It can be seen that the inhibition efficiency reaches a maximum value at optimum concentration (200 ppm) of vanillin.

Effect of immersion time

To study the effect of immersion time, SDPS plots obtained from current noise signals of two AA6061 electrodes with different surface areas after 1 h, 24h, 48h and 72h from immersion time and during 300 s in 3.5% NaCl solution in the presence of optimum concentration of vanillin are shown in Fig. 5. Table 4 shows the noise parameters obtained from SDPS plots. It is evident that the quantity of electric charge was decreased with

increasing immersion time. This may be ascribed to adsorption of vanillin molecules over the corroded surface [17].

The adsorption of vanillin is increased with increasing immersion time and thereby the inhibition is improved.

Table 2. Polarization parameters and the corresponding inhibition efficiency values for AA6061 in 3.5% NaCl containing different concentrations of vanillin

C/ppm	-E _{corr} /mV	i _{corr} /nA.cm ⁻²	b _a /(mV/dec)	b _c /(mV/dec)	IE%
0	690	1560	36	495	-
100	689	549	20	321	65
200	707	186	21	204	88
500	696	436	23	296	72
1000	693	544	23	372	65

Table 3. Noise parameters and the corresponding inhibition efficiency values for AA6061 in 3.5% NaCl containing different concentrations of vanillin

C./ppm	d _{max}	Δt/s	i _{max} /nA	Q/nCoul	IE%
0	d4	3	9.7	29.1	-
100	d2	0.8	6.6	5.0	82
200	d2	0.8	3.2	2.4	91
500	d3	1.5	3.0	4.5	84
1000	d4	3	4.4	13.2	55

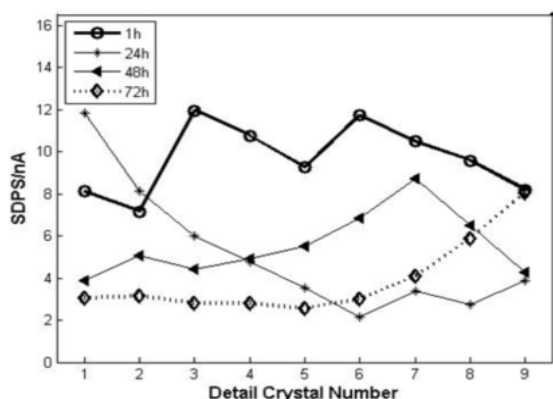


Fig. 5. SDPS plots obtained from current noise signals of 200 ppm vanillin in 3.5% NaCl solution for different immersion times.

Quantum chemical calculations

Quantum molecular descriptors

Quantum molecular parameters are useful to predict the potential of the inhibitor molecules to interact with surface metal atoms. Most effective corrosion inhibitors

are usually those organic compounds that can offer electrons to unoccupied orbital of the metal, and also accept free electrons from the metal [18]. Then inhibitor with higher HOMO level energy has more tendency to offer electrons to unoccupied orbital of the aluminum, and thereby shows the higher the corrosion inhibition efficiency. In addition, decrease in the LUMO–HOMO energy gap can improve the efficiency of inhibitor. Quantum chemical parameters listed in Table 5 reveal that vanillin has high HOMO and low LUMO with high energy gap (molecular orbital plots of vanillin are shown in Fig. 6).

Table 4. Noise parameters for AA6061 in 3.5% NaCl in the presence of 200 ppm vanillin after various times from immersion time

Time/h	Crystal	Δt/s	SDPS/nA	Q/nCoul
1	d3	1.5	12	18
24	d1	0.4	11.8	4.7
48	d2	0.8	5.0	4.0
72	d2	0.8	3.2	2.6

The bonding tendencies of the inhibitors towards the metal atom can be discussed in terms of the HSAB (hard-soft-acid-base) concept. General rule suggested by the principle of HSAB, is that hard acids

prefer to coordinate to hard bases and soft acids prefer to coordinate to soft bases. On the other hand, metal atoms are known as soft acids. Hard molecules have a high HOMO–LUMO gap and soft molecules have a small HOMO–LUMO gap, and thus soft bases inhibitors are the most effective for metals that is 3.3519 a.u for vanillin.

Table 5. Quantum molecular descriptors of vanillin, Al surface and vanillin...Al. All values are in units of (a.u.)

Molecular descriptors	vanillin
Total energy	-535.2388
E_{HOMO}	-0.2354
E_{LUMO}	-0.0629
$E_{\text{LUMO}} - E_{\text{HOMO}}$	0.1725
$I = -E_{\text{HOMO}}$	0.2354
$A = -E_{\text{LUMO}}$	0.0629
$\eta = (I-A)/2$	0.0863
$S = 1/2 \eta$	3.3519
$\mu = -(I+A)/2$	-0.1492
$\chi = -\mu$	0.1492
$\omega = \mu^2/2 \eta$	0.1289
$\Delta N = \frac{\chi_{\text{Al}} - \chi_{\text{vanillin}}}{2(\eta_{\text{Al}} - \eta_{\text{vanillin}})}$	0.1180

I = ionization potential, A = electron affinity

Furthermore, the number of transferred electrons was also calculated that is the fraction of electrons transferred from inhibitor to the aluminum surface. Values of ΔN showed inhibition effect resulted by electrons donation from vanillin to aluminum.

Fukui indices

Local reactivity was analyzed by the Fukui indices (FI), since they indicated the reactive regions. This depicts the atoms which are responsible for bond formation [19]. The results of Mulliken population analysis, Table 6, show the charge distribution of vanillin. The results of Table 6 for vanillin molecule show higher Fukui indices (f^-) in oxygen atoms that mean oxygen atoms of vanillin are strongest donor sites.

NBO analysis

NBO calculations were performed in order to study the interactions between the filled orbitals of inhibitor molecule and the vacant orbitals of aluminum. The stabilization energy, $E^{(2)}$, provides a quantitative standard of the strength of the interaction between an electron donor and the receptor. With greater $E^{(2)}$, there is a stronger interaction between the electron donor orbital and receptor orbital [20, 21]. According to the Table 7, the data show that the calculated stabilization energy, $E^{(2)}$, for the interaction of vanillin with aluminum surface is mainly due to the interaction with the unoccupied valance nonbonding orbital of aluminum. The greatest $E^{(2)}$ values appear in the valance lone pair of carbonyl oxygen to unoccupied valance nonbonding of aluminum interactions with a stabilization energy of 109.12 kcal/mol.

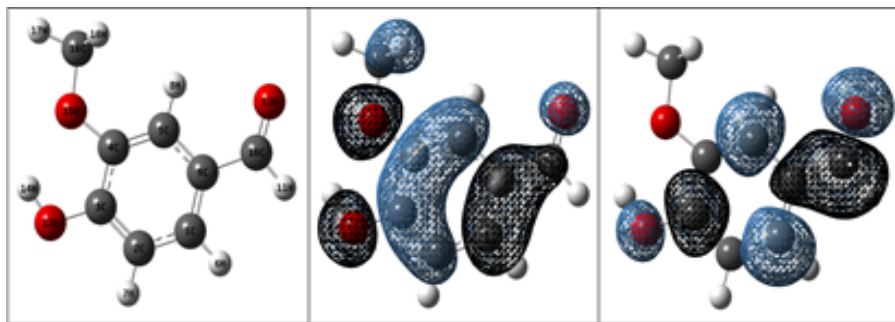


Fig. 6. Optimized structure and molecular orbital plots for Vanillin using LanL2DZ.

QTAIM investigation

To investigate the effect of concentration on activity of vanillin, the intermolecular hydrogen bonding in vanillin systems were analyzed by AIM method. The AIM descriptors of vanillin, vanillin...vanillin (five different orientations of two molecules) and vanillin... vanillin... vanillin (three orientations of three molecules) complexes are given in Table 8 and AIM molecular graphs of these complexes are shown in Fig. 7. The all Laplacians and electronic energy densities are positive except these of O¹³...H¹⁴ (H<0) bond in vanillin...V 2 complex and O¹⁵...H¹⁴ (H<0) bond in vanillin...V 5 complex. Two topological parameters both the total electron density H_{BCP} and Laplacian at BCP ($\nabla^2\rho_{BCP}$) were used to classified the interaction to strong hydrogen bond (covalent nature: $\nabla^2\rho_{BCP}<0$ and H_{BCP} <0), medium hydrogen bond}

(partially covalent nature: $\nabla^2\rho_{BCP} >0$ and H_{BCP} <0) and weak hydrogen bond (mainly electrostatic nature: $\nabla^2\rho_{BCP} >0$ and H_{BCP} >0) [22, 23]. Therefore, interactions for molecular systems studied here have a partially covalent nature (medium strength) in O¹³...H¹⁴ and O¹⁵...H¹⁴ interactions but mainly electrostatic nature in other intermolecular interactions of vanillin.}}

The results of AIM, Fukui indices and NBO show that all reactive atoms of vanillin having main role of interaction with aluminum surface can be reactive by intermolecular hydrogen bonds. It can be observed from Table 8 and Fig. 7 that the number of intermolecular hydrogen bonds can be increased by increase in concentration of vanillin. These results can verify the decrease in corrosion inhibition efficiency of vanillin at high concentrations.

Table 6. The calculated Mulliken charges and Fukui indices for atoms in vanillin

atom	q ^(N-1)	q ^(N)	q ^(N+1)	f ⁺	f ⁻
C ¹	-0.319	-0.384	-0.460	0.076	0.065
C ²	-0.256	-0.304	-0.346	0.042	0.048
C ³	0.203	0.150	0.074	0.076	0.053
C ⁴	0.325	0.260	0.225	0.035	0.065
C ⁵	-0.436	-0.489	-0.607	0.118	0.053
H ⁶	0.295	0.241	0.202	0.039	0.054
H ⁷	0.316	0.260	0.207	0.053	0.056
H ⁸	0.325	0.287	0.263	0.024	0.038
C ⁹	0.489	0.449	0.463	-0.014	0.040
C ¹⁰	-0.151	-0.197	-0.363	0.166	0.046
H ¹¹	0.213	0.171	0.098	0.073	0.042
O ¹²	-0.137	-0.227	-0.372	0.145	0.090
O ¹³	-0.318	-0.442	-0.501	0.059	0.124
H ¹⁴	0.432	0.391	0.355	0.036	0.041
O ¹⁵	-0.295	-0.367	-0.383	0.016	0.072
C ¹⁶	-0.488	-0.479	-0.477	-0.002	-0.009
H ¹⁷	0.281	0.237	0.199	0.038	0.044
H ¹⁸	0.261	0.223	0.211	0.012	0.038
H ¹⁹	0.261	0.223	0.211	0.012	0.038

Table 7. Some invaluable second-order interaction energies ($E^{(2)}$, kcal/mol) of vanillin...Al interaction

Donor	Acceptor	$E^{(2)}$	$E_{(j)} - E_{(i)}$	F_{ij}
LP(1) _{O15}	LP*(4) _{Al}	7.55	0.53	0.066
BD(1) _{C5-C9}	LP*(4) _{Al}	3.74	0.73	0.056
BD(1) _{C9-C1}	LP*(4) _{Al}	4.11	0.73	0.058
BD(2) _{C9-C1}	LP*(4) _{Al}	5.77	0.29	0.039
BD(1) _{C9-C10}	LP*(4) _{Al}	3.22	0.65	0.049
LP(1) _{O13}	LP*(3) _{Al}	4.95	0.57	0.056
LP(3) _{O13}	LP*(3) _{Al}	3.99	0.58	0.044
BD(1) _{C9-C10}	LP*(3) _{Al}	5.36	0.65	0.059
BD(1) _{C10-O12}	LP*(3) _{Al}	9.35	1.03	0.099
BD(2) _{C10-O12}	LP*(3) _{Al}	12.03	0.40	0.069
BD(1) _{C16-H 17}	LP*(3) _{Al}	5.22	0.58	0.059
LP(1) _{O12}	LP*(3) _{Al}	26.08	0.69	0.132

Items with the highest energy gain were selected.

LP: Valance Lone Pair

BD: Two-Center Bond

LP*: Unoccupied Valance Nonbonding

Table 8. AIM (BCP) topological descriptors of the vanillin intermolecular interactions

	Bond	ρ	G	V	H	$\nabla^2\rho$
vanillin	O ¹⁵ ...H ¹⁴	0.0203	0.0215	-0.0183	0.0032	0.0986
vanillin...v 1	H ¹⁷ ...O ¹²	0.0125	0.0109	-0.0085	0.0024	0.0530
vanillin...v 2	O ¹⁵ ...H ¹⁷	0.0103	0.0084	-0.0065	0.0019	0.0410
	O ¹³ ...O ¹⁵	0.0158	0.0159	-0.0123	0.0037	0.0785
	O ¹³ ...H ¹⁴	0.0431	0.0398	-0.0415	-0.0017	0.1522

Table 8. Continue						
vanillin...v 3	O ¹² ...H ¹⁷	0.0004	0.0003	-0.0002	0.0001	0.0015
	H ¹⁸ ...C ⁵	0.0017	0.0009	-0.0006	0.0004	0.0051
	C ³ ...C ³	0.0012	0.0006	-0.0004	0.0002	0.0036
	C ² ...O ¹³	0.0010	0.0007	-0.0004	0.0002	0.0036
	C ⁴ ...C ⁴	0.0014	0.0007	-0.0004	0.0003	0.0037
vanillin...v 4	O ¹² ...H ¹¹	0.0094	0.0082	-0.0059	0.0023	0.0422
	O ¹² ...H ⁶	0.0105	0.0095	-0.0069	0.0026	0.0484
vanillin...v 5	O ¹³ ...H ¹⁷	0.0078	0.0064	-0.0046	0.0018	0.0328
	H ¹⁷ ...O ¹⁵	0.0127	0.0116	-0.0090	0.0026	0.0568
	O ¹⁵ ...O ¹⁵	0.0098	0.0085	-0.0067	0.0018	0.0415
	O ¹⁵ ...H ¹⁴	0.0424	0.0398	-0.0413	-0.0015	0.1532
v...vanillin...v 1	O ¹³ ...C ²	0.0009	0.0006	-0.0003	0.0002	0.0032
	H ⁷ ...C ¹⁶	0.0012	0.0008	-0.0004	0.0004	0.0049
	H ⁶ ...H ¹⁸	0.0009	0.0006	-0.0003	0.0003	0.0035
	H ⁷ ...H ⁷	0.0007	0.0004	-0.0002	0.0002	0.0024
	H ¹⁹ ...H ⁶	0.0039	0.0027	-0.0014	0.0012	0.0158
v...Vanillin...v 2	O ¹³ ...H ⁶	0.0004	0.0003	-0.0002	0.0001	0.0017
	H ¹⁷ ...H ¹¹	0.0012	0.0008	-0.0004	0.0003	0.0044
	H ¹⁸ ...C ⁴	4.65×10 ⁵	3.56×10 ⁵	-1.74×10 ⁵	1.82×10 ⁵	0.0002
	O ¹² ...H ¹⁸	0.0040	0.0030	-0.0019	0.0011	0.0163
	O ¹² ...H ¹⁹	0.0002	0.0002	-9.04×10 ⁵	8.51×10 ⁵	0.0010
	H ⁶ ...O ¹²	0.0015	0.0011	-0.0001	0.0004	0.0061
	H ¹¹ ...O ¹²	0.0023	0.0018	-0.0010	0.0007	0.0099
v...Vanillin...v 3	O ¹² ...H ⁷	0.0125	0.0104	-0.0083	0.0021	0.0499
	H ¹¹ ...O ¹³	0.0124	0.0108	-0.0086	0.0022	0.0524
	O ¹⁵ ...H ⁶	0.0122	0.0106	-0.0083	0.0023	0.0518
	H ¹⁴ ...C ¹	0.0057	0.0044	-0.0030	0.0014	0.0230

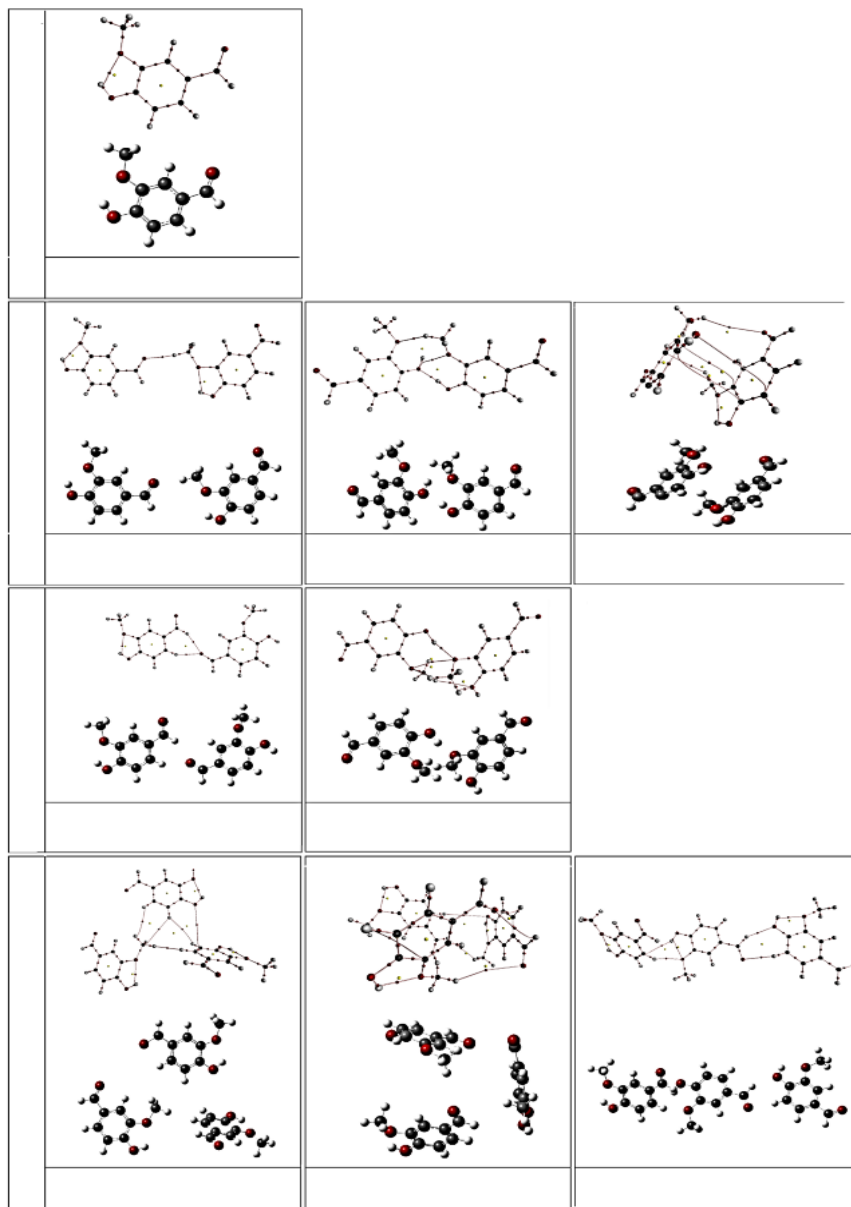


Fig. 7. Optimized structures and AIM molecular graphs of (a) vanillin (b) vanillin...vanillin (c) vanillin...vanillin...vanillin.

CONCLUSIONS

The inhibition effect of vanillin on the corrosion behavior of AA6061 in 3.5% NaCl was studied using electrochemical techniques. Due to nontoxicity properties and high solubility in aqueous media, vanillin offers interesting possibilities for corrosion inhibition. According to calculated amount of noise charges by

using the standard deviation of partial signal (SDPS) at the particular interval of frequency it is possible to obtain the inhibition efficiency of an inhibitor. The IE values obtained from EN data of vanillin show a reasonable agreement with those obtained from potentiodynamic polarization measurements.

It can be deduced from quantum chemical calculations that the number of intermolecular hydrogen bonds is increased by increase in the concentration of vanillin. This proves the decrease in the inhibition efficiency of vanillin in high concentrations.

REFERENCES

- [1]. R. Salghi, L. Bazzi, B. Hammouti, A. Bendou, E.A. Addi and S. Kertit, *Prog. Org. Coat.*, 51 (2004) 113.
- [2]. A.J. Aldykewicz, H.S. Isaacs and A.J. Davenport, *J. Electrochem. Soc.*, 142 (1995) 3342.
- [3]. V. Guillaumin and G. Mankowski, *Corros. Sci.*, 41 (1999) 421.
- [4]. K.A. Yasakau, M.L. Zheludkevich, O.V. Karavai and M.G.S. Ferreira, *Prog. Org. Coat.*, 63 (2008) 352.
- [5]. G. Gece, *Corros. Sci.*, 53 (2011) 3873.
- [6]. P.B. Raja and M.G. Sethuraman, *Mater. Lett.*, 62 (2008) 113.
- [7]. N.J. Walton, M.J. Mayer and A. Narbad, *Phytochemistry*, 63 (2003) 505.
- [8]. Y. Li, R. Hu, J. Wang, Y. Huang and C.-J. Lin, *Electrochim. Acta*, 54 (2009) 7134.
- [9]. [9] J.A. Wharton, R.J.K. Wood and B.G. Mellor, *Corros. Sci.*, 45 (2003) 97.
- [10]. A. Aballe, M. Bethencourt, F.J. Botana and M. Marcos, *Electrochem. Commun.*, 1 (1999) 266.
- [11]. M. Shahidi, S.M.A. Hosseini and A.H. Jafari, *Electrochim. Acta*, 56 (2011) 9986.
- [12]. M.J. Frisch and e. al., *Gaussian 03, Revision B.03*, in, *Gaussian, Inc.*, Pittsburgh PA, 2003.
- [13]. E.G. Lewars, *Computational Chemistry: Introduction to the Theory and Applications of Molecular and Quantum Mechanics*, Springer, 2010.
- [14]. T.C. Allison and Y.J. Tong, *Electrochim. Acta*, 101 (2013) 334.
- [15]. C.F. Matta and R.J. Boyd, *The Quantum Theory of Atoms in Molecules: From Solid State to DNA and Drug Design*, in, *Wiley-VCH*, Germany, 2007.
- [16]. G. Golestani, M. Shahidi and D. Ghazanfari, *Appl. Surf. Sci.*, 308 (2014) 347.
- [17]. A.Y. El-Etre, *Corros. Sci.*, 43 (2001) 1031.
- [18]. P. Zhao, Q. Liang and Y. Li, *Appl. Surf. Sci.*, 252 (2005) 1596.
- [19]. M. Oftadeh, N.M. Mahani and M. Hamadian, *Res. Pharm. Sci.*, 8 (2013) 285.
- [20]. F. Weinhold and C.R. Landis, *Valency and Bonding, A Natural Bond Orbital Donor–Acceptor Perspective*, Cambridge University Press, Cambridge, 2005.
- [21]. F. Weinhold and C.R. Landis, *Discovering Chemistry With Natural Bond Orbitals*, Wiley, New Jersey, 2012.
- [22]. A. Fonari, E.S. Leonova and M.Y. Antipin, *Polyhedron*, 30 (2011) 1710.
- [23]. R.N. Singh, A. Kumar, R.K. Tiwari, P. Rawat and V.P. Gupta, *J. Mol. Struct.*, 1035 (2013) 427.